

Spatial heterogeneity of aerosol effect on liquid cloud microphysical properties in the warm season over Tibetan Plateau

Pengguo Zhao^{1, 2}, Wen Zhao³, Liang Yuan¹, Xin Zhou¹, Fei Ge¹, Hui Xiao⁴, Peiwen Zhang², Yuting Wang¹, Yunjun Zhou¹

1. Plateau Atmosphere and Environment Key Laboratory of Sichuan Province, College of Atmospheric Science, Chengdu University of Information Technology, Chengdu, China

2. Institute of Plateau Meteorology, China Meteorological Administration, Chengdu, China

3. School of Cybersecurity, Chengdu University of Information Technology, Chengdu, China

4. Guangzhou Institute of Tropical and Marine Meteorology, China Meteorological Administration, Guangzhou, China

Corresponding author: Pengguo Zhao (zpg@cuit.edu.cn)

Key Points:

- The effect of aerosol on liquid cloud is spatially disparate between the southern (STP) and northern Tibetan Plateau (NTP).
- Positive relationship between the aerosol index (AI) and the liquid cloud droplet effective radius (LREF) is shown in both STP and NTP.
- LREF first increases and then decreases in the STP while always increases in the NTP with the increase of AI.

Abstract

The effect of aerosol on liquid cloud microphysical properties over the Tibetan Plateau during the warm season is investigated by employing aerosol index and cloud property parameters. Distinct differences in aerosol effect on liquid cloud microphysical properties have been found between the northern TP (NTP) and southern TP (STP). The composite liquid cloud droplet effective radius (LREF) anomalies for positive aerosol index (AI) events are positive in the NTP and negative in the STP. In both NTP and STP, when the AI anomalies are positive, the LREF anomalies are also positive, which suggests that the increased aerosol loading reduces the solar radiation reaching the ground and thus enhances the atmospheric stability, making cloud droplets not conducive to break up. This indicates that the aerosol radiative effect is not likely the reason causing the distinct differences of aerosol effects on liquid cloud properties between NTP and STP. Further analysis shows that in the STP, the LREF first increases and then decreases with the increase of AI, while in the NTP, the LREF always increases with the increase of AI, suggesting a spatial difference in aerosol microphysical effect. In the STP, the influence of aerosol on liquid clouds is mainly dependent

on liquid water path (LWP) and convective available potential energy (CAPE), while in the NTP, the influence of aerosol on liquid cloud is more likely related to large aerosol particles.

Plain Language Summary

This study indicates that the influence of aerosol on liquid cloud over the TP is spatially different. AI is positively correlated with LREF in the NTP and STP, which is due to the aerosol radiation effect. Since the aerosol microphysical effect depends on local environmental conditions, in the STP, the LREF increases first and then decreases with the increase of AI, and in the NTP, the LREF always increases with AI.

1. Introduction

Aerosol-radiation-interaction (ARI) and aerosol-cloud-interaction (ACI) are still prominent uncertainty sources in climate change assessment (IPCC, 2021). Aerosol directly scatters and absorbs solar radiation through radiative effect (Chylek and Wong, 1995; Penner et al., 1992), and indirectly affects cloud macro- and micro- physical properties and precipitation processes as cloud condensation nucleus (CCN) through microphysical effect (Garrett and Zhao, 2006; Rosenfeld et al., 2014; Rotstajn, 1999; Twomey, 1977; Zhao et al., 2018).

The influence of aerosol on liquid cloud properties is mainly manifested in the effect of aerosol acting as CCN on cloud droplet size and number concentration. When the liquid water content (LWC) is steady, the increase of aerosol would lead to the formation of more smaller cloud droplets, known as the “Twomey effect” (Twomey, 1977). Previous observational and simulation studies (Fan et al., 2020; Garrett et al., 2004; Khain and Pokrovsky, 2014; Koren et al., 2005; Liu et al., 2017; Penner et al., 2014; Rosenfeld et al., 2014; Wang et al., 2015; Werner et al., 2014; Zhang et al., 2012; Zhao et al., 2012) have verified the hypothesis that the increase of aerosol leads to the decrease of cloud droplet size. However, some studies have found that there is an anti-Twomey effect, that is, the increase of aerosol leads to the increase in cloud droplet size (Grandey and Stier, 2010; Ma et al., 2018; Sekiguchi et al., 2003; Yuan et al., 2008; Wang et al., 2014; 2015). This anti-Twomey effect is speculated to be related to weakly soluble aerosols, insufficient water supply, stable atmosphere, stratiform cloud regimes, and so on (Gryspeerdt and Stier, 2012; Qiu et al., 2017; Yuan et al., 2008; Wang et al., 2014). Ma et al. (2018) found that aerosol is positively correlated with cloud droplet size in the industrial regions, but negatively in the adjacent ocean regions. It is suggested that the positive correlation is associated with low stability and high cloud top, while the negative correlation is associated with low cloud top with high stability. There are still uncertainties and local differences in aerosol-cloud interactions. It has been figured out that clouds are more sensitive to aerosol forcing in relatively clean regions (Garrett and Zhao, 2006; Qiu et al., 2017; Zhao et al., 2020). As one of the remote clean regions on the Earth, what is the relationship between aerosols and clouds over the Tibetan Plateau (TP)?

The TP, also known as the Water Tower of Asia, influences the large-scale atmospheric circulation and the water cycle of the Asian continent through its dynamic and thermal forcing (Wu et al., 2007; Ye and Wu, 1998). Observational evidence indicated significant warming over the TP (Duan and Xiao, 2015; He et al., 2003; Kulkarni et al., 2002). Under the background of global warming, the influence of aerosols on weather and climate over the TP has attracted increasing attentions.

Many studies have shown the significance of aerosols on the weather and climate over the TP. Huang et al. (2006; 2007) indicated that dust storms occur frequently over the TP, especially on the northern slope of the TP, and found that dust aerosols reduce cloud water path through the semi-direct effect. Lua et al. (2010) found that dust and black carbon aerosols contribute to widespread warming and accelerate snow melt over the TP by heating the atmosphere. Jia et al. (2018) employed satellite observations to suggest that dust aerosols affect the radiation energy budget and atmospheric thermodynamic structure significantly over the Tibetan Plateau by affecting the shortwave radiation process. Liu et al. (2019) suggested that with the increase of aerosol over the TP, the ice cloud effective radius decreases significantly during the daytime but change weakly at nighttime, and the ice water path decreases slightly during the daytime while increases significantly at nighttime. Zhao et al. (2020) indicated that anthropogenic aerosols from South Asia and dust aerosols from the Taklimakan Desert could influence weather and climate over the TP and downstream through their effects on radiation balance and cloud processes. Hua et al. (2020) combined satellite observations with CMIP5 model products and found that the response of ice clouds to aerosol indirect effect is more sensitive than that of liquid clouds over TP, resulting in a more significant effect of aerosol on the radiative forcing of ice clouds than that of liquid clouds.

In this study, we use the aerosol and cloud properties data, along with the ERA5 reanalysis to investigate the spatial heterogeneity in aerosol effect on the liquid cloud over the TP. The data and methods are presented in section 2, the potential linkage of aerosol with the liquid cloud over the TP is discussed in section 3, and the conclusions are summarized in section 4.

2. Data and methodology

In this study, the aerosol, cloud, and meteorological datasets from 1995 to 2015 are used to investigate the effect of aerosol on the microphysical properties of liquid cloud during the warm season over the TP.

2.1. Aerosol

The aerosol index (AI) is defined as aerosol optical depth (AOD) times Ångström exponent (AE), which is a better characterization of aerosol number concentration than AOD because it takes aerosol size information into account (Penner et al., 2011; Stier, 2016). The AI is used in this study to examine the effect of aerosol particles as cloud condensation nuclei on cloud microphysical properties, especially for fine mode aerosol particles (Nakajima et al., 2001; Ma et al., 2018).

AODs and AEs or different types of aerosols are provided by the Modern-Era Retrospective analysis for Research and Applications, version 2 (MERRA-2) aerosol dataset, with an original spatial resolution of $0.5^\circ \times 0.625^\circ$ (Randles et al., 2017; Buchard et al., 2017). To match the cloud properties data set, aerosol products were interpolated into a spatial resolution of $0.25^\circ \times 0.25^\circ$. Sun et al. (2019a; 2019b) evaluated the MERRA-2 reanalysis aerosol products over China using satellite and ground-based observations and found that the MEERA-2 aerosol products have a good agreement with the observed aerosol products. Thus, MERRA-2 AOD and AE observations can be used in this study with reliable quality. Actually, the MEERA-2 aerosol products have already been used in previous studies (Liu et al., 2019; Hua et al., 2019) regarding the potential effect of aerosol on liquid and ice clouds over the TP.

2.2. Cloud properties

The CM SAF cloud, albedo and surface radiation dataset from the AVHRR data, edition 2 (CLARA-A2) provided the monthly cloud properties with a spatial resolution of $0.25^\circ \times 0.25^\circ$ (Karlsson et al., 2017). The reliability of CLARA-A2 has been evaluated by previous studies and the CLARA-A2 has been adopted in various studies. Karlsson et al. (2017) and Karlsson and Håkansson (2018) used MODIS and Pathfinder Atmosphere Extended (PATMOS-x) cloud products to compare with the CLARA-A2 cloud products and found a good agreement. Liu et al. (2020) evaluated the CLARA-A2 cloud products by using the MODIS products and applied it to the study regarding the capacity of clouds to produce precipitation over Central and East Asia. Zhao et al. (2022) employed the CLARA-A2 cloud products to examine the cloud microphysical precipitation efficiency over the TP.

Cloud properties including the cloud fraction (CF), the cloud top pressure (CTP), the cloud optical thickness (τ), the liquid cloud droplet effective radius (LREF), and the liquid water path (LWP) are selected for this study. CDNC is obtained from τ and LREF, according to the following formula (Bennartz, 2007; Bai et al., 2018; Quaas et al., 2006),

$$CDNC = \alpha \tau^{0.5} LREF^{-2.5},$$

where $\alpha = 1.37 \times 10^{-5} m^{-0.5}$. Note that the CDNC is estimated based on the assumption that the cloud vertical structure follows the classical adiabatic growth theory (Quaas et al., 2006).

2.3. Meteorology

The uncertainty of aerosol effects on cloud and precipitation is highly dependent on the meteorological conditions (Li et al., 2011; Han et al., 2022; Stevens and Feingold, 2009). Previous studies (Bai et al., 2018; Filioglou et al., 2019; Ma et al., 2018; Matsui et al., 2004) used the lower-tropospheric static stability (LTS), defined as the potential temperature difference between the sea level and 700 hPa, to describe the thermodynamic condition in the study of aerosol effect on the cloud. For the Tibetan Plateau with an average altitude of more than 4000

m, the convective available potential energy (CAPE) is more suitable to characterize the thermal stability of the atmosphere. In this study, monthly CAPEs from 1995 to 2015 were obtained from the ERA5 reanalysis dataset with a spatial resolution of $0.25^\circ \times 0.25^\circ$ (Dee et al., 2011). Freychet et al. (2019) evaluated the relative humidity, dry-bulb temperature, and wet-bulb temperature of the ERA5 reanalysis dataset by using the ground-based observation dataset over China and found a good consistency.

3. Results

3.1. AI and cloud properties over the TP

The main part of the TP examined in this study refers to the area with an elevation of more than 2000 m. Since the local anthropogenic emissions of atmospheric pollutants over the TP are relatively small, the aerosol loading is significantly lower than that in its surrounding areas and other continental areas at the same latitude (Liao et al., 2021; Liu et al., 2015; Xia et al., 2021; Zhu et al., 2019). The transport of atmospheric pollutants from the surrounding areas to the TP is an important contribution to the local aerosols over the TP (Li et al., 2020; Zhao et al., 2020). Figure 1 shows the changing trend of the AI and the time series of the standardized AI anomaly over the TP from 1995 to 2015. As shown in Figure 1a, AI shows a consistent upward trend throughout the TP from 1995 to 2015. The variation range of AI in the main body of the TP was small, approximately $1 \times 10^{-4} \text{ month}^{-1}$. The aerosols over southern and eastern parts of the TP were affected by surrounding areas, and the increased range of AI was larger, approximately $3 \times 10^{-4} \text{ month}^{-1}$. The time series of the AI anomaly over the TP is created by removing the annual cycle and linear trend and standardizing. As shown in Figure 1b, we select 0.5 as the positive threshold as an indicator to represent the larger AI events (hereafter called positive events), and -0.5 as the negative threshold to represent the smaller AI events (hereafter called negative events).

There are obvious seasonal differences in cloud properties over the TP (Fujinami and Yasunari, 2001; Wang et al., 2015; Yang et al., 2020; Zhao et al., 2019), so we focus on the warm season to investigate the influence of aerosol on liquid cloud properties. Figure 2 shows the composite LREF and CDNC anomalies for AI positive and negative events in the warm season over the TP. The LREF anomalies for positive events have obvious spatial differences over the TP (Figure 2a). Specifically, the influence of aerosols on cloud droplet effective radius has a distinct north-south difference. In the northern TP (NTP), more aerosols lead to a larger LREF, while in the southern TP (SNT), more aerosols lead to a smaller radius. According to the Twomey effect, for constant liquid water content, an increase in aerosol concentration leads to the formation of more smaller cloud droplets (Twomey, 1977). It is interesting to note that the aerosol effect on LREF shows a Twomey effect in the SNT, while in the NTP, there is an anti-Twomey effect. Previous observational studies (Bulgin et al., 2008; Liu et al., 2017; Ma et al., 2018; Sekiguchi et al., 2003; Tang et al., 2014) also found a similar anti-Twomey effect over various regions, which is likely associated with

local meteorological conditions, cloud regimes, and aerosol microphysics. The composite LREF anomalies for negative events (Figure 2b) are not as significant as those for positive events. In the NTP, the LREF is smaller when there is less aerosol, while in the STP, the change of LREF is not obvious when the aerosol is less. This may be related to much lower aerosol loading over the TP than other regions. The CDNC anomalies for positive and negative events (Figures 2c and 2d) show opposite patterns compared to the LREF anomalies. It suggests that in the NTP, the increase of aerosol leads to the increase of LREF and decrease of CDNC; and in the STP, the increase of aerosol leads to the decrease of LREF and increase of CDNC.

The effect of aerosol on clouds is recognized as a very complex physical process, which is usually influenced by aerosol microphysics, cloud regime, and meteorological conditions, such as vertical velocity, wind shear, and stability of the lower atmosphere (Gryspeerd et al., 2016; Lee et al., 2014; Lehahn et al., 2011; Li et al., 2011; Rosenfeld et al., 2014; Yang et al., 2019). The difference in meteorological conditions between the STP and the NTP is obvious (Yao et al., 2008; Yu et al., 2008), while aerosols in the STP and the NTP are contributed by aerosol transport from different regions, causing significant differences in aerosol properties between the two regions (Yang et al., 2021; Zhao et al., 2020). The influence of aerosol on LREF and CDNC is opposite over the NTP and STP, which may be related to the differences in both meteorological conditions and aerosol microphysics between the NTP and STP.

The CFs as a function of CTP over the NTP and STP in the warm season are shown in Figures 3a and 3b, in which cloud properties are classified into 6 groups according to the AI, with the same sample size in each group. Previous studies (Koren et al., 2005; Li et al., 2011; Saponaro et al., 2017) have suggested that an increase in aerosol loading over both ocean and land regions could enhance cloud vertical development. An increase in aerosols also contributes to the increase in cloud coverage by reducing cloud droplet sizes (Gryspeerd et al., 2016; Kaufman and Koren, 2006; Rosenfeld et al., 2019). It is found that aerosol influences both cloud top height and cloud fraction over the NTP and STP. The CF (also CTP) corresponding to the group with lowest AI values is smaller than that corresponding to the groups with higher AI values over the NTP and STP. They indicate that aerosol increase contributes to the cloud formation and vertical development, which is evident over the NTP and STP.

Figures 3c and 3d show CFs as a function of CTP under different CAPE conditions. According to low, medium, and high CAPE, cloud properties are classified into three groups with the same sample size in each group. An unstable atmosphere is conducive to cloud formation and development. The CF and cloud top height corresponding to the group with lowest CAPE values are significantly smaller than that corresponding to the groups with higher CAPE values. The CAPE excitation effect on cloud is more evident over the STP, which may be due to more abundant water vapor and more unstable thermal conditions over the STP than that over the NTP in the warm season.

The occurrence frequency of CAPE and CTP over the NTP and STP in the warm season is presented in Figure 4. The occurrence frequency of CAPE and CTP is significantly different between the NTP and the STP. The CAPE over the NTP is significantly smaller than that over the STP. During the warm season, the cases with CAPE values of approximately 100 J kg^{-1} are most frequent in the NTP, while that with CAPE values of more than 200 J kg^{-1} are more frequent in the STP. The CTP over the STP (approximately 250 hPa to 450 hPa) is more widely distributed than that over the NTP (approximately 320 hPa to 450 hPa). Although the cases with CTP of approximately 380 hPa are the most frequent over the STP and the NTP, the clouds with higher cloud top are more frequent over the STP than over the NTP, which is related to the stronger unstable energy (Figure 4a) and more abundant moisture over the STP (Jiang and Ting, 2017; Yao et al., 2013).

3.2. Effects of aerosol on liquid cloud over the NTP and STP

Results in Figure 2 have already indicated that aerosol has a positive effect on the cloud droplet effective radius over the NTP, but the opposite effect over the STP. Further analysis is needed to determine whether the effect of aerosol on cloud droplets is monotonous over the TP. Figure 5 shows the variation of LREF and CDNC anomalies with AI anomaly over the STP and NTP in the warm season. Over both STP and NTP, when AI anomalies are less (larger) than 0, most LREF anomalies are less (larger) than 0 m, especially the mean values, suggesting that whether in the STP or NTP, the cloud droplet effective radius is larger (smaller) when the aerosol loading is larger (smaller). This phenomenon may be related to the consistent radiative effects of aerosols in both the STP and NTP. Aerosols scatter and absorb solar radiation through the radiation effect, reducing the solar radiation reaching the surface, thus reducing the near-surface temperature, and enhancing the stability of the lower troposphere (Guleria et al., 2014; Li et al., 2022; Yang et al., 2017). For the TP with poor thermodynamic conditions (Figure 4) and weak convection prevailing (Jiang and Fan, 2002; Fu et al., 2006) in the warm season, relatively low near-surface temperature and relatively stable lower atmosphere are not conducive to the development of convection. Correspondingly, the updraft movement, and horizontal and vertical cloud development will be weak (Figure 3c and 3d), so that the cloud droplets grown by condensation are not easy to be broken up, making LREF larger.

Differently, with the increase of aerosol loading, the cloud droplet effective radius first increases and then decreases over the STP (Figure 5a), while over the NTP, the cloud droplet effective radius always increases (Figure 5b). The difference in cloud droplet effective radius variation with aerosol between the STP and NTP is speculated to be caused by the different performance of aerosol microphysical effect on liquid cloud, which is highly related to the thermodynamic conditions, moisture and liquid water content, and aerosol properties over the STP and NTP.

The average state of aerosol loading over the TP is lower than that in the surrounding regions, especially in the STP (Jia et al., 2015; Liu et al., 2019; Zhao

et al., 2020). When the aerosol loading in the STP (Figure 5a) is lower than its average state (AI anomaly < 0), the increase of AI leads to the increase of LREF, which is because, in the case of extremely low aerosol concentration, there are not enough cloud condensation nuclei to activate and form cloud droplets. Once the aerosol increases, relatively more cloud droplets will form in the cloud, which is conducive to the collision-coalescence process between cloud droplets, leading to the increase of the cloud droplet effective radius. When the aerosol loading in the STP is higher than its average state (AI anomaly > 0), the increase of AI leads to the decrease of LREF. In this case, more CCN activate to form more cloud droplets, and numerous smaller cloud droplets compete for the quasi-constant liquid water, resulting in a decrease in cloud droplet effective radius.

Over the NTP (Figure 5b), when the aerosol loading is lower than its average state (AI anomaly < 0), the cloud droplet effective radius increases with the increase of aerosol, but the trend is not obvious, the reason for which is worthy for further investigation in future. When the aerosol loading is higher than its average state (AI anomaly > 0), the cloud droplet effective radius increases with the increase of aerosol evidently. This may be related to the dominant role of dust aerosols with larger particle size in the NTP, the activation of giant CCN to form large cloud droplets, and the increase of aerosols will promote the increase of the cloud droplet effective radius.

The CDNC anomaly (Figure 5c and 5d) change with AI anomaly is opposite to the change of LREF anomaly. Due to the aerosol radiation effect, in the STP and NTP, the CDNC is higher (lower) than the average state when AI is lower (higher) than the average state. In the STP, the CDNC first decreases and then increases with the increase of AI, while in the NTP, the CDNC always decreases with the increase of AI.

We hypothesize that aerosol influence on LREF and CDNC is consistent between the STP and NTP due to the aerosol radiative effect. To further verify this hypothesis, the change of CDNC anomaly with CAPE in the warm season is shown in Figure 6. CDNC shows a significant trend of first rising and then decreasing with the change of CAPE over the STP and NTP. In the case of lower CAPE, the cloud fraction is less, and cloud top height is lower (Figures 3c and 3d). The CDNC increases with the increase of CAPE, which confirms the hypothesis of aerosol radiative effect proposed above (Figures 5c and 5d). According to the hypothesis, in the STP and NTP, aerosols reduce the solar radiation reaching the ground and enhance the stability of the lower troposphere. Stronger stability (lower CAPE) is not conducive to the fragmentation of cloud droplets, and LREF increases through condensation and CDNC decreases.

When CAPE is relatively large, in the STP and NTP, CDNC decreases with the increase of CAPE, which may be due to the fact that strong convection and updraft movement are conducive to the widening of cloud droplet spectrum and the occurrence of cloud droplet collision-coalescence, leading to the decrease of CDNC.

LWP plays an important role in adjusting the influence of aerosol on cloud microphysics (McCoy et al., 2020). Figure 7 shows the variations of LREF anomaly with AI anomaly under different LWP conditions over the STP and NTP. Over the STP, the correlations between AI anomaly and LREF anomaly are weak under low and medium LWP conditions, while a positive correlation between AI anomaly and LREF anomaly is obvious under high LWP conditions. Over the NTP, the dependence of the influence of AI on LREF on LWP conditions is not evident. There are significant positive correlations between AI anomaly and LREF anomaly under both low and high LWP conditions. Ma et al. (2018) found that with the increase of LWP, the positive correlations between aerosol and cloud droplet effective radius get weakened over land, while the negative correlations change slightly over the ocean. Under the lower LWP and cloud optical depth conditions, the cloud and precipitation susceptibilities to aerosol perturbation are more prominent in the warm marine clouds (Bai et al., 2018; Terai et al., 2012). Over the TP, AI influence on LREF is noticeable at high LWP, probably due to the compression effect of the plateau topography on clouds causing liquid clouds to be thinner than that in other regions (Yan et al., 2016; Zhao et al., 2022). In thinner liquid clouds, the aerosol-cloud interaction cannot be revealed under low LWP conditions.

Due to the unique local moisture and the thermodynamic environment caused by the tall topography of the TP, weak convective clouds dominate the warm season in this region (Fujinami and Yasunari, 2001; Kurosaki and Kimura, 2002). CAPE was adopted to represent the local thermodynamic conditions of the TP in this study. Figure 8 shows the variation of LREF anomaly varies with AI anomaly under different CAPE conditions over the STP and NTP. Over the STP (Figure 8a), AI and LREF show a significant positive correlation under low CAPE conditions, but the effect of aerosol on cloud droplet effective radius is not visible under medium and high CAPE conditions. Over the STP, the response of CF and CTP to CAPE is very sensitive, with low CAPE corresponding to low CF and high CTP (Figure 3d). Under relatively stable conditions, cloud bodies have weak horizontal and vertical development. By consuming water vapor, aerosols hygroscopically grow and activate to form cloud droplets, which continue to grow by condensation. Over the NTP, AI and LREF are positively correlated under different CAPE conditions, and the correlation is also most significant under low CAPE conditions. The effect of CAPE on CF and CTP over the NTP is not as significant as that over the STP, and the correlation between AI and LREF over the NTP (Figure 8b) is not as dependent on high LWP and low CAPE conditions as it is over the STP.

The influence of aerosol on cloud microphysical processes is dependent on the aerosol microphysics, such as particle size, chemical composition, and mixing state, because aerosol microphysics determines the activation process of aerosol directly (Bhattu and Tripathi, 2015; Paramonov et al., 2013). Since it is difficult to obtain aerosol microphysics at a regional scale (Ma et al., 2018), AE is selected to characterize aerosol particle size indirectly in this study. Low AE represents the relatively larger aerosols. Figure 9 shows the variation of LREF

anomaly with AI anomaly under different AE conditions over the STP and NTP. Over the STP, there is a significant positive correlation between AI and LREF for relatively large aerosol particles (low AE), but there are no significant correlations between AI and LREF for medium and high AE conditions. Over the NTP, AI shows a significant correlation with LREF under both low and high AE conditions. The AE in the NTP is significantly smaller than that in the STP (Figure S1), suggesting that the aerosol size in the NTP is larger than that in the STP. For the NTP, the overall large aerosol size makes the influence of aerosol on cloud droplet effective radius independent of aerosol particle size, because larger aerosol particles are more conducive to activation (Ji and Shaw, 1998; Snider et al., 2003). While, for the STP where the overall aerosol size is small, relatively larger aerosols could be more easily activated to form cloud droplets and thus affect the liquid cloud. In other words, the influence of aerosol on cloud droplet effective radius in the STP depends on aerosol particle size.

The influence of aerosol on LREF through the microphysical effect is spatially different between the STP and NTP, which may be associated with the thermodynamic conditions, cloud regime, and aerosol size. Over the NTP, the CAPE is smaller, the cloud top height is lower, the cloud height range is smaller, and the aerosol particle size is larger. The aerosol has a positive influence on the cloud droplet effective radius, which may be due to the larger aerosol particles and relatively uniform cloud regime. Over the STP, the CAPE is larger, the cloud top height is higher, and the cloud height range is larger. The cloud droplet effective radius increases first and then decreases with the increase of aerosol, which may be related to local thermodynamic conditions and cloud regime.

4. Discussion and Conclusions

Based on 21-year aerosol, cloud, and meteorology data from 1995 to 2015, the influence of aerosol on liquid cloud microphysical properties in the warm season over the TP is investigated.

The influence of aerosol on the microphysical properties of liquid cloud in the warm season has spatial disparity according to the composite LREF anomalies and CDNC anomalies. Over the NTP, when the aerosol loading is higher, the LREF is larger and the CDNC is lower; on the contrary, over the STP, when the aerosol loading is higher, the LREF is smaller and the CDNC is higher. In other words, the aerosol has a positive effect on the LREF over the NTP, while there is a negative correlation over the STP.

Similarly, over the STP and NTP, when the AI is larger than its average state, the LREF is larger than its average state, and vice versa. This is likely associated with the aerosol radiative effect. When the aerosol loading is higher over the TP, the solar radiation reaching the ground is reduced, enhancing the stability of the lower troposphere that is not conducive to convective development and updraft, which makes cloud droplets less likely to break up and continue to grow through condensation. Previous studies (Guleria et al., 2014; Li et al., 2022; Yang et al., 2017) have also confirmed that aerosols increase the stabil-

ity of the lower atmosphere through radiative effects. For the TP with weak thermodynamic conditions, the LREF increases, and CDNC decreases with the decrease of CAPE under the stable condition.

Over the STP, the effect of aerosol on the LREF is not monotonous. LREF first increases and then decreases with the increase of AI. The anti-Twomey effect of LREF with aerosol may be related to the extremely low aerosol loading over the TP. Once the aerosol increases, the aerosol will rapidly activate and form cloud droplets, promoting the collision-coalescence process and increasing the size of cloud droplets. As aerosols continue to increase, more cloud condensation nuclei compete for water vapor, increasing the concentration of cloud droplets and decreasing the effective radius. While, over the NTP, LREF always shows an increasing trend with the increase of AI, especially when AI is higher than its average state. This may be because the aerosol particle size is large, and the cloud regime is relatively uniform over the NTP. The increase of aerosol leads to the formation of large cloud droplets in the cloud, which is conducive to the increase of LREF.

The difference in the influence of aerosol on LREF and CDNC between the NTP and STP is largely due to the differences in thermodynamic conditions, cloud regimes, and the aerosol particle size between the two regions. The thermodynamic conditions in the STP are stronger than those in the NTP, the cloud height range is larger than that in the NTP, and the aerosol particle size is smaller than that in the NTP. Studies on the physical mechanism should be combined with modeling studies in the future.

Acknowledgments

This research was jointly supported by the National Natural Science Foundation of China (42075086 and 41905126), and the Sichuan Science and Technology Program (2021YJ0393), and the Second Tibetan Plateau Scientific Expedition and Research (STEP) program (2019QZKK0104).

Data Availability Statement

MERRA-2 aerosol data can be download from <https://disc.sci.gsfc.nasa.gov/MERRA/>, the ERA5 data are from <https://cds.climate.copernicus.eu/>, and the CLARA-A2 data are from https://wui.cmsaf.eu/safira/action/viewDoiDetails?acronym=CLARA_AVHRR_V002.

References

- Bai, H., Gong, C., Wang, M., Zhang, Z., L'Ecuyer, T. (2018), Estimating precipitation susceptibility in warm marine clouds using multi-sensor aerosol and cloud products from A-Train satellites. *Atmospheric Chemistry and Physics*, 18, 1763–1783. <https://doi.org/10.5194/acp-18-1763-2018>
- Bennartz, R. (2007), Global assessment of marine boundary layer cloud droplet number concentration from satellite. *Journal of Geophysical Research: Atmospheres*, 112(D2), D02201. <https://doi.org/10.1029/2006JD007547>

- Bhattu, D., Tripathi, S. N. (2015), CCN closure study: Effects of aerosol chemical composition and mixing state. *Journal of Geophysical Research: Atmospheres*, 120, 766–783. <https://doi.org/10.1002/2014JD021978>
- Buchard, V., Randles, C. A., Da Silva, A. M., Darmenov, A., Colarco, P. R., Govindaraju, R., Ferrare, R., Hair, J., Beyersdorf, A. J., Ziemba, L. D., Yu, H. (2017), The MERRA-2 aerosol reanalysis, 1980 onward, Part II: Evaluation and case studies. *Journal of Climate*, 30, 6851–6872. <https://doi.org/10.1175/JCLI-D-16-0613.1>
- Bulgin, C. E., Palmer, P. I., Thomas, G. E., Arnold, C. P., Campmany, E., Carboni, E., Lawrence, B. N. (2008), Regional and seasonal variations of the Twomey indirect effect as observed by the ATSR-2 satellite instrument. *Geophysical Research Letters*, 35, L02811. <https://doi.org/10.1029/2007GL031394>
- Chen Q., Fan J., Yin Y., Han B. (2020), Aerosol impacts on mesoscale convective systems forming under different vertical wind shear conditions. *Journal of Geophysical Research: Atmospheres*, 125, e2018JD030027. <https://doi.org/10.1029/2018JD030027>
- Chylek, P., Wong J. (1995), Effect of absorbing aerosols on global radiation budget. *Geophysical Research Letters*, 22, 929–931. <https://doi.org/10.1029/95GL00800>
- Dee, D. P., Uppala, S. M., Simmons, A. J., Berrisford, P., Poli, P., Kobayashi, S., Andrae, U., Balmaseda, M. A., Balsamo, G., Bauer, P., Bechtold, P., Beljaars, A. C. M., van de Berg, L., Bidlot, J., Bormann, N., Delsol, C., Dragani, R., Fuentes, M., Geer, A. J., Haimberger, L., Healy, S. B., Hersbach, H., Hólm, E. V., Isaksen, I., Kållberg, P., Köhler, M., Matricardi, M., McNally, A. P., Monge-Sanz, B. M., Morcrette, J. J., Park, B. K., Peubey, C., de Rosnay, P., Tavolato, C., Thépaut, J. N., Vitart, F. (2011), The ERA-Interim reanalysis: Configuration and performance of the data assimilation system. *Quarterly Journal of the Royal Meteorological Society*, 137, 553–597. <https://doi.org/10.1002/qj.828>
- Duan, A., Xiao, Z. (2015), Does the climate warming hiatus exist over the Tibetan Plateau? *Revstat-Statistical journal*, 5, 13711. <https://doi.org/10.1038/srep13711>
- Filioglou, M., Mielonen, T., Balis, D., Giannakaki, E., Arola, A., Kokkola, H., Komppula, M., Romakkaniemi, S. (2019), Aerosol effect on the cloud phase of low-level clouds over the Arctic. *Journal of Geophysical Research: Atmospheres*, 124, 7886–7899. <https://doi.org/10.1029/2018JD030088>
- Fu, Y., Liu, G., Wu, G., Yu, R., Xu, Y., Wang, Y., Li, R., Liu, Q. (2006), Tower mast of precipitation over central Tibetan plateau summer. *Geophysical Research Letters*, 33, L05802. <https://doi.org/10.1029/2005GL024713>
- Fujinami, H., Yasunari, T. (2001), The seasonal and intraseasonal variability of diurnal cloud activity over the Tibetan plateau. *Journal of the Meteorological Society of Japan*, 79, 1207–1227. <https://doi.org/10.2151/jmsj.79.1207>
- Freychet, N., Tett, S. F. B., Yan, Z., Li, Z. (2020), Underestimated change of wet-bulb temperatures over East and South China. *Geophysical Research*

Letters, 47, e2019GL086140. <https://doi.org/10.1029/2019GL086140>

Garrett, T. J., Zhao, C., Dong, X., Mace, G. G., Hobbs, P. V. (2004), Effects of varying aerosol regimes on low-level Arctic stratus. *Geophysical Research Letters*, 31, L17105. <https://doi.org/10.1029/2004gl019928>

Garrett, T. J., Zhao, C. (2006), Increased Arctic cloud longwave emissivity associated with pollution from mid-latitudes. *Nature*, 440, 787–789. <https://doi.org/10.1038/nature04636>.

Guleria, R. P., Kuniyal, J. C., Dhyani, P. P., Joshi, R., Sharma, N. L. (2014), Impact of aerosol on surface reaching solar irradiance over Mohal in the north-western Himalaya, India. *Journal of Atmospheric and Solar-terrestrial Physics*, 108, 41–49. <https://doi.org/10.1016/j.jastp.2013.12.002>

Gryspeerdt, E., Quaas, J., Bellouin, N. (2016), Constraining the aerosol influence on cloud fraction. *Journal of Geophysical Research: Atmospheres*, 121, 3566–3583. <https://doi.org/10.1002/2015JD023744>.

Gryspeerdt, E., Stier, P. (2012), Regime-based analysis of aerosol-cloud interactions. *Geophysical Research Letters*, 39, L21802. <https://doi.org/10.1029/2012GL053221>

Han, X., Zhao, B., Lin, Y., Chen, Q., Shi, H., Jiang, Z., Fan, X., Wang, J., Liou, K., Gu, Y. (2022), Type-dependent impact of aerosols on precipitation associated with deep convective cloud over East Asia. *Journal of Geophysical Research: Atmospheres*, 127, e2021JD036127. <https://doi.org/10.1029/2021JD036127>

He, Y., Zhang, Z., Theakstone, W. H., Chen, T., Yao, T., Pang, H. (2003), Changing features of the climate and glaciers in China’s monsoonal temperate glacier region. *Journal of Geophysical Research: Atmospheres*, 108(D17), 4530. <https://doi.org/10.1029/2002JD003365>

Hua, S., Liu, Y., Luo, R., Shao, T., Zhu, Q. (2020), Inconsistent aerosol indirect effects on water clouds and ice clouds over The Tibetan Plateau. *International Journal of Climatology*, 40, 3832–3848. <https://doi.org/10.1002/joc.6430>

Huang, J., Lin, B., Minnis, P., Wang, T., Wang, X., Hu, Y., Yi, Y., Ayers, K. (2006), Satellite-based assessment of possible dust aerosols semi-direct effect on cloud water path over East Asia. *Geophysical Research Letters*, 33, L19802. <https://doi.org/10.1029/2006GL026561>

Huang, J., Minnis, P., Yi, Y., Tang, Q., Wang, X., Hu, Y., Liu, Z., Ayers, K., Trepte, C., Winker, D. (2007), Summer dust aerosols detected from CALIPSO over the Tibetan Plateau. *Geophysical Research Letters*, 34, L18805. <https://doi.org/10.1029/2007GL029938>

IPCC. (2021), Climate change 2021: the physical science basis. <https://www.ipcc.ch/report/ar6/wg1/download>

Ji, Q., Shaw, G. E. (1998), On supersaturation spectrum and size distributions of cloud condensation nuclei. *Geophysical Research Letters*, 25, 1903–1906. <https://doi.org/10.1029/98GL01404>

- Jia, H., Ma, X., Yu, F., Liu, Y., Yin, Y. (2019), Distinct impacts of increased aerosols on cloud droplet number concentration of stratus/stratocumulus and cumulus. *Geophysical Research Letters*, 46, 13517–13525. <https://doi.org/10.1029/2019GL085081>
- Jia, R., Liu, Y., Hua, S., Zhu, Q., Shao, T. (2018), Estimation of the aerosol radiative effect over the Tibetan Plateau based on the latest Calipso product. *Journal of Meteorological Research*, 32, 707–722. <https://doi.org/10.1007/s13351-018-8060-3>
- Jia, R., Liu, Y., Chen, B., Zhang, Z., Huang, J. (2015), Source and transportation of summer dust over the Tibetan Plateau. *Atmospheric Environment*, 123, 210–219. <https://doi.org/10.1016/j.atmosenv.2015.10.038>
- Jiang, J., Fan, M. (2002), Convective clouds and mesoscale convective systems over the Tibetan plateau in summer. *Chinese Journal of Atmospheric Sciences*, 26, 263–270. <https://doi.org/10.3878/j.issn.1006-9895.2002.02.12>
- Jiang, X., Ting, M. (2017), A dipole pattern of summertime rainfall across the Indian Subcontinent and the Tibetan Plateau. *Journal of Climate*, 30, 9607–9620. <https://doi.org/10.1175/JCLI-D-16-0914.1>
- Karlsson, K. G., Anttila, K., Trentmann, J., Stengel, M., Meirink, J. F., Devasthale, A. (2017), CLARA-A2: the second edition of the CM SAF cloud and radiation data record from 34 years of global AVHRR data. *Atmospheric Chemistry and Physics*, 17, 5809–5828. <https://doi.org/10.5194/acp-17-5809-2017>
- Karlsson, K. G., Håkansson, N. (2018), Characterization of AVHRR global cloud detection sensitivity. *Atmospheric Chemistry and Physics*, 11, 633–649. <https://doi.org/10.5194/amt-11-633-2018>
- Kaufman, Y. J., Koren, I. (2006), Smoke and pollution aerosol effect on cloud cover. *Science*, 313, 655–658. <https://doi.org/10.1126/science.1126232>
- Khain, A. P., Pokrovsky, A. (2004), Simulation of effects of atmospheric aerosols on deep turbulent convective clouds using a spectral microphysics mixed-phase cumulus cloud model. Part II: sensitivity study. *Journals of the Atmospheric Sciences*, 61, 2983–3001. <https://doi.org/10.1175/JAS-3350.1>
- Klein, S. A., Hartmann, D. L. (1993), The seasonal cycle of low stratiform clouds. *Journal of Climate*, 6, 1587–1606. [https://doi.org/10.1175/1520-0442\(1993\)006%3C1587:TSCOLS%3E2.0.CO;2](https://doi.org/10.1175/1520-0442(1993)006%3C1587:TSCOLS%3E2.0.CO;2)
- Koren, I., Kaufman, Y. J., Rosenfeld, D., Remer, L. A., Rudich, Y. (2005), Aerosol invigoration and restructuring of Atlantic convective clouds. *Geophysical Research Letters*, 32, L14828. <https://doi.org/10.1029/2005GL023187>
- Kurosaki, Y., Kimura, F. (2002), Relationship between topography and daytime cloud activity around Tibetan plateau. *Journal of The Meteorological Society of Japan*, 80, 1339–1355. <https://doi.org/10.2151/jmsj.80.1339>

- Kulkarni, A. V., Mathur, P., Rathore, B. P., Alex, S., Thakur, N., Kumar, M. (2002), Effect of global warming on snow ablation pattern the Himalayas. *Current Science*, 83(2), 120–123.
- Lau, W. K. M., Kim, M. K., Kim, K. M., Lee, W. S. (2010), Enhanced surface warming and accelerated snow melt in the Himalayas and Tibetan Plateau induced by absorbing aerosols. *Environmental Research Letters*, 5, 025204. <https://doi.org/10.1088/1748-9326/5/2/025204>
- Lee, S. S., Kim, B. G., Lee, C., Yum, S. S., Posselt, D. (2014), Effect of aerosol pollution on clouds and its dependence on precipitation intensity. *Climate Dynamics*, 42, 557–577. <https://doi.org/10.1007/s00382-013-1898-2>
- Lehahn, Y., Koren, I., Altaratz, O., Kostinski, A. B. (2011), Effect of coarse marine aerosols on stratocumulus clouds. *Geophysical Research Letters*, 38, L20804. <https://doi.org/10.1029/2011GL048504>, 2011
- Li, F., Wan, X., Wang, H., Orsolini, Yvan J., Cong, Z., Gao, Y., Kang, S. (2020), Arctic sea-ice loss intensifies aerosol transport to the Tibetan Plateau. *Nature Climate Change*, 10, 1037–1044. <https://doi.org/10.1038/s41558-020-0881-2>
- Li, J., Carlson, B. E., Yung, Y. L., Lv, D., Hansen, J., Penner, J. E., Liao, H., Ramaswamy, V., Kahn, R. A., Zhang, P., Dubovik, O., Ding, A., Lacis, A. A., Zhang, L., Don, Y. (2022), Scattering and absorbing aerosols in the climate system. *Nature Reviews Earth & Environment*, 3, 363–379. <https://doi.org/10.1038/s43017-022-00296-7>
- Li, Z., Niu, F., Fan, J., Liu, Y., Rosenfeld, D., Ding, Y. (2011), Long-term impacts of aerosols on the vertical development of clouds and precipitation. *Nature Geoscience*, 4, 888–894. <https://doi.org/10.1038/ngeo1313>
- Liao, T., Gui, K., Li, Y., Wang, X., Sun, Y. (2021), Seasonal distribution and vertical structure of different types of aerosols in southwest China observed from CALIOP. *Atmospheric Environment*, 246, 118145. <https://doi.org/10.1016/j.atmosenv.2020.118145>
- Liu, Y., Sato, Y., Jia, R., Xie, Y., Huang, J., Nakajima, T. (2015), Modeling study on the transport of summer dust and anthropogenic aerosols over the Tibetan Plateau. *Atmospheric Chemistry and Physics*, 15, 12581–12594. <https://doi.org/10.5194/acp-15-12581-2015>
- Liu, Y., Leeuw, G. D., Kerminen, V. M., Zhang, J., Zhou, P., Nie, W., Qi, X., Hong, J., Wang, Y., Ding, A., Guo, H., Kruger, O., Kulmala, M., Petaja, T. (2017), Analysis of aerosol effects on warm clouds over the Yangtze River Delta from multi-sensor satellite observations. *Atmospheric Chemistry and Physics*, 17, 5623–5641. <https://doi.org/10.5194/acp-17-5623-2017>
- Liu, Y., Hua, S., Jia, R., Huang, J. (2019), Effect of aerosols on the ice cloud properties over the Tibetan Plateau. *Journal of Geophysical Research: Atmospheres*, 124, 9594–9608. <https://doi.org/10.1029/2019JD030463>

- Liu, Y., Luo, R., Zhu, Q., Hua, S., Wang, B. (2020), Cloud ability to produce precipitation over arid and semiarid regions of Central and East Asia. *International Journal of Climatology*, 40, 1824–1837. <https://doi.org/10.1002/joc.6304>
- Ma, X., Jia, H., Yu, F., Quaas, J. (2018), Opposite aerosol index-cloud droplet effective radius correlations over major industrial regions and their adjacent oceans. *Geophysical Research Letters*, 45, 5771–5778. <https://doi.org/10.1029/2018GL077562>
- Matsui, T., H.Masunaga, R. A., Pielke S., Tao, W. K. (2004), Impact of aerosols and atmospheric thermodynamics on cloud properties within the climate system. *Geophysical Research Letters*, 31, L06109. <https://doi.org/10.1029/2003GL019287>
- McCoy, D. T., Field, P., Gordon, H., Elsaesser, G. S., Grosvenor, D. P. (2020), Untangling causality in midlatitude aerosol–cloud adjustments. *Atmospheric Chemistry and Physics*, 20, 4085–4103. <https://doi.org/10.5194/acp-20-4085-2020>
- Nakajima, T., Higurashi, A., Kawamoto, K., Penner, J. E. (2001), A possible correlation between satellite-derived cloud and aerosol microphysical parameters. *Geophysical Research Letters*, 28, 1171–1174. <https://doi.org/10.1029/2000GL012186>
- Paramonov, M., Aalto, P. P., Asmi, A., Prisle, N., Kerminen, V. M., Kulmala, M., Petäjä, T. (2013), The analysis of size-segregated cloud condensation nuclei counter (CCNC) data and its implications for cloud droplet activation. *Atmospheric Chemistry and Physics*, 13, 10285–10301. <https://doi.org/10.5194/acp-13-10285-2013>
- Penner, J. E., Dickinson, R. E., O'Neill, C. A. (1992), Effects of aerosol from biomass burning on the global radiation budget. *Science*, 256, 1432–1434. <https://doi.org/10.1126/science.256.5062.1432>
- Penner, J. E., Dong, X., Chen, Y. (2004), Observational evidence of a change in radiative forcing due to the indirect aerosol effect. *Nature*, 427, 231–234. <https://doi.org/10.1038/nature02234>
- Penner, J. E., Xu, L., Wang, M. (2011), Satellite methods underestimate indirect climate forcing by aerosols. *Proceedings of the National Academy of Sciences*, 108, 13404–13408. <https://doi.org/10.1073/pnas.1018526108>
- Qiu, Y., Zhao C., Guo, J., Li, J. (2017), 8-Year ground-based observational analysis about the seasonal variation of the aerosol-cloud droplet effective radius relationship at SGP site. *Atmospheric Environment*, 164, 139–146. <https://doi.org/10.1016/j.atmosenv.2017.06.002>
- Quaas, J., Boucher, O., Lohmann, U. (2006), Constraining the total aerosol indirect effect in the LMDZ and ECHAM4 GCMs using MODIS satellite data. *Atmospheric Chemistry and Physics*, 6, 947–955. <https://doi.org/10.5194/acp-6-947-2006>

- Randles, C. A., Da Silva, A. M., Buchard, V., Colarco, P. R., Darmenov, A., Govindaraju, R., Smirnov, A., Holben, B., Ferrare, R., Hair, J., Shinozuka, Y. (2017), The MERRA-2 aerosol reanalysis, 1980 onward. Part I: System description and data assimilation evaluation. *Journal of Climate*, 30, 6823–6850. <https://doi.org/10.1175/JCLI-D-16-0609.1>
- Ryohei, M., Yasushi, U., Kazuhiko, M., Tatsuhiko, M., Yutaka, T., Yoko, I. (2022), Classification of aerosol-cloud interaction regimes over Tokyo. *Atmospheric Research*, 272. <https://doi.org/10.1016/j.atmosres.2022.106150>
- Rosenfeld, D., Sherwood, S., Wood, R., Donner, L. (2014), Climate effects of aerosol-cloud interactions. *Science*, 343, 379–380. <https://doi.org/10.1126/science.1247490>
- Rosenfeld, D., Zhu, Y., Wang, M., Zheng, Y., Goren, T., Yu, S. (2019), Aerosol-driven droplet concentrations dominate coverage and water of oceanic low-level clouds. *Science*, 363, 599. <https://doi.org/10.1126/science.aav0566>
- Rosenfeld, D., Andreae, M. O., Asmi, A., Chin, M., de Leeuw, G., Donovan, D. P., Kahn, R., Kinne, S., Kivekäs, N., Kulmala, M., Lau, W., Schmidt K. S., Suni, T., Wagner, T., Wild, M., Quaas, J. (2014), Global observations of aerosol-cloud-precipitation-climate interactions. *Reviews of Geophysics*, 52, 750–808. <https://doi.org/10.1002/2013RG000441>
- Rotstayn, L. D. (1999), Indirect forcing by anthropogenic aerosols: A global climate model calculation of the effective-radius and cloud-lifetime effects. *Journal of Geophysical Research: Atmospheres*, 104, 9369–9380. <https://doi.org/10.1029/1998JD900009>
- Saponaro, G., Kolmonen, P., Sogacheva, L., Rodriguez, E., Virtanen, T., Leeuw, G. D. (2017), Estimates of the aerosol indirect effect over the Baltic Sea region derived from 12 years of MODIS observations. *Atmospheric Chemistry and Physics*, 17(4), 3133–3143. <https://doi.org/10.5194/acp-17-3133-2017>
- Sekiguchi, M., Nakajima, T., Suzuki, K., Kawamoto, K., Higurashi, A., Rosenfeld, D., Sano, I., Mukai, S. (2003), A study of the direct and indirect effects of aerosols using global satellite data sets of aerosol and cloud parameters. *Journal of Geophysical Research: Atmospheres*, 108(D22), 4699. <https://doi.org/10.1029/2002JD003359>
- Snider, J. R., Guibert, S., Brenguier, J. L., Putaud, J. P. (2003), Aerosol activation in marine stratocumulus clouds: 2. Köhler and parcel theory closure studies. *Journal of Geophysical Research: Atmospheres*, 108(D15), 8629, <https://doi.org/10.1029/2002JD002692>
- Stevens, B., Feingold, G. (2009), Untangling aerosol effects on clouds and precipitation in a buffered system. *Nature*, 461, 607–613. <https://doi.org/10.1038/nature08281>
- Stier, P. (2016), Limitations of passive remote sensing to constrain global cloud condensation nuclei. *Atmospheric Chemistry and Physics*, 16(10), 6595–6607. <https://doi.org/10.5194/acp-16-6595-2016>

- Sun, E., Che, H., Xu, X., Wang, Z., Lu, C., Gui, K., Zhao, H., Zheng, Y., Wang, Y., Wang, H., Sun, T. (2019), Variation in MERRA-2 aerosol optical depth over the Yangtze River Delta from 1980 to 2016. *Theoretical and Applied Climatology*, 136, 363–375. <https://doi.org/10.1007/s00704-018-2490-9>
- Sun, E., Xu, X., Che, H., Tang, Z., Gui, K., An, L., Lu, C., Shi, G. (2019), Variation in MERRA-2 aerosol optical depth and absorption aerosol optical depth over China from 1980 to 2017, *Journal of Atmospheric and Solar-Terrestrial Physics*, 186, 8–19. <https://doi.org/10.1016/j.jastp.2019.01.019>
- Tang, J., Wang, P., Mickley, L. J., Xia, X., Liao, H., Yue, X. (2014), Positive relationship between liquid cloud droplet effective radius and aerosol optical depth over Eastern China from satellite data. *Atmospheric Environment*, 84, 244–253. <https://doi.org/10.1016/j.atmosenv.2013.08.024>
- Terai, C. R., Wood, R., Leon, D. C., Zuidema, P. (2012), Does precipitation susceptibility vary with increasing cloud thickness in marine stratocumulus? *Atmospheric Chemistry and Physics*, 12, 4567–4583. <https://doi.org/10.5194/acp-12-4567-2012>
- Tsarpalis, K., Katsafados, P., Papadopoulos, A., Mihalopoulos, N. (2020), Assessing Desert Dust Indirect Effects on Cloud Microphysics through a Cloud Nucleation Scheme: A Case Study over the Western Mediterranean, *Remote Sensing*, 12, 1–26. <https://doi.org/10.3390/rs12213473>
- Twomey, S. (1977), The influence of pollution on the shortwave albedo of clouds. *Journals of The Atmospheric Sciences*, 34(7), 1149–1152. [https://doi.org/10.1175/1520-0469\(1977\)34<1149:TIOP>2.0.CO;2](https://doi.org/10.1175/1520-0469(1977)34<1149:TIOP>2.0.CO;2)
- Wang, C., Shi, H., Hu, H., Wang, Y., Xi, B. (2015), Properties of cloud and precipitation over the Tibetan Plateau. *Advances in Atmospheric Sciences*, 32, 1504–1516. <https://doi.org/10.1007/s00376-015-4254-0>
- Wang, F., Guo, J., Wu, Y., Zhang, X., Deng, M., Li, X., Zhang, J., Zhao, J. (2014), Satellite observed aerosol-induced variability in warm cloud properties under different meteorological conditions over eastern China. *Atmospheric Environment*, 84, 122–132. <https://doi.org/10.1016/j.atmosenv.2013.11.018>
- Wang, F., Guo, J., Zhang, J., Huang, J., Min, M., Chen, T., Liu, H., Deng, M., Li, X. (2015), Multi-sensor quantification of aerosol-induced variability in warm cloud properties over eastern China. *Atmospheric Environment*, 113, 1–9. <https://doi.org/10.1016/j.atmosenv.2015.04.063>
- Werner, F., Ditas, F., Siebert, H., Simmel, M., Wehner, B., Pilewskie, P., Schmeissner, T., Shaw, R. A., Hartmann, S., Wex, H., Roberts, G. C., Wendisch, M. (2014), Twomey effect observed from collocated microphysical and remote sensing measurements over shallow cumulus. *Journal of Geophysical Research: Atmospheres*, 119, 1534–1545. <https://doi.org/10.1002/2013JD020131>
- Wu, G., Liu, Y., Zhang, Q., Duan, A., Wang, T., Wan, R., Liu, X., Li, W., Wang, Z., Zhang, Q., Duan, A., Liang, X. (2007), The influence of mechan-

- cal and thermal forcing by the Tibetan Plateau on Asian climate. *Journal of Hydrometeorology*, 8(4), 770–789. <https://doi.org/10.1175/JHM609.1>
- Xia, X., Che, H., Shi, H., Chen, H., Zhang, X., Wang, P., Goloub, P., Holben, B. (2021), Advances in sunphotometer-measured aerosol optical properties and related topics in China: Impetus and perspectives. *Atmospheric Research*, 249, 105286. <https://doi.org/10.1016/j.atmosres.2020.105286>
- Yao, T., Duan, K., Xu, B., Wang, N., Guo, X., Yang, X. (2008), Precipitation record since ad 1600 from ice cores on the central Tibetan plateau. *Climate of the Past*, 4(3), 175–180.
- Yao, T., Masson-Delmotte, V., Gao, J., Yu, W., Yang, X., Risi, C., Sturm, C., Werner, M., Zhao, H., He, Y., Ren, W., Tian, L., Shi, C., Hou, S. (2013), A review of climatic controls on $\delta^{18}O$ in precipitation over the Tibetan Plateau: observations and simulations. *Reviews of Geophysics*, 51(4), 525–548. <https://doi.org/10.1002/rog.v51.4>
- Yan, Y., Liu, Y., Lu, J. (2016), Cloud vertical structure, precipitation, and cloud radiative effects over Tibetan Plateau and its neighboring regions. *Journal of Geophysical Research: Atmospheres*, 121, 5864–5877. <https://doi.org/10.1002/2015JD024591>
- Yang, J., Duan, K., Kang, S., Shi, P., Ji, Z. (2017), Potential feedback between aerosols and meteorological conditions in a heavy pollution event over the Tibetan Plateau and Indo-Gangetic Plain. *Climate Dynamics*, 48, 2901–2917. <https://doi.org/10.1007/s00382-016-3240-2>
- Yang, X., Yao, Z., Li, Z., Fan, T. (2013), Heavy air pollution suppresses summer thunderstorms in central China. *Journal of Atmospheric and Solar-Terrestrial Physics*, 95, 28–40. <https://doi.org/10.1016/j.jastp.2012.12.023>
- Yang, X., Li, Z., Liu, L., Zhou, L., Cribb, M., Zhang, F. (2016), Distinct weekly cycles of thunderstorms and a potential connection with aerosol type in China. *Geophysical Research Letters*, 43, 8760–8768. <https://doi.org/10.1002/2016GL070375>
- Yang, Y., Zhao, C., Dong, X., Fan, G., Zhou, Y., Wang, Y., Zhao, L., Lv, F., Yan, F. (2019), Toward understanding the process-level impacts of aerosols on microphysical properties of shallow cumulus cloud using aircraft observations. *Atmospheric Research*, 221, 27–33. <https://doi.org/10.1016/j.atmosres.2019.01.027>
- Yang, Y., Zhao, C., Fan, H. (2020), Spatiotemporal Distributions of Cloud Properties Over China Based on Himawari-8 Data. *Atmospheric Research*, 240, 104927. <https://doi.org/10.1016/j.atmosres.2020.104927>
- Yang, Y., Zhao, C., Wang, Q., Cong, Z., Yang, X., Fan, H. (2021), Aerosol characteristics at the three poles of the Earth as characterized by Cloud–Aerosol Lidar and Infrared Pathfinder Satellite Observations. *Atmospheric Chemistry and Physics*, 21, 6, 4849–4868. <https://doi.org/10.5194/acp-21-4849-2021>

- Ye, D., Wu, G. (1998), The role of the heat source of the Tibetan Plateau in the general circulation. *Archives for Meteorology, Geophysics, and Bioclimatology, Series A*, 67, 181–198. <https://doi.org/10.1007/BF01277509>
- Yu, W., Yao, T., Tian, L., Ma, Y., Ichianagi, K., Wang, Y., Sun, W. (2008), Relationships between ^{18}O in precipitation and air temperature and moisture origin on a south-north transect of the Tibetan Plateau. *Atmospheric Research*, 87(2), 158–169. <https://doi.org/10.1016/j.atmosres.2007.08.004>
- Yuan, T., Li, Z., Zhang, R., Fan, J. (2008), Increase of cloud droplet size with aerosol optical depth: An observation and modeling study. *Journal of Geophysical Research: Atmospheres*, 113, D04201. <https://doi.org/10.1029/2007JD008632>
- Zhao, C., Tie, X., Lin, Y. (2006), A possible positive feedback of reduction of precipitation and increase in aerosols over eastern central China. *Geophysical Research Letters*, 33, L11814. <https://doi.org/10.1029/2006GL025959>
- Zhao, C., Klein, S. A., Xie, S., Liu, X., Boyle, J. S., Zhang, Y. (2012), Aerosol First Indirect effects on non-precipitating low-level liquid cloud properties as simulated by CAM5 at ARM sites. *Geophysical Research Letters*, 39, L08806. <https://doi.org/10.1029/2012GL051213>
- Zhao, C., Qiu, Y., Dong, X., Wang, Z., Peng, Y., Li, B., Wu, Z., Wang, Y. (2018), Negative aerosol-cloud r_e relationship from aircraft observations over Hebei, China. *Earth and Space Science*, 5, 19–29. <https://doi.org/10.1002/2017EA00034>
- Zhao, C., Chen, Y., Li, J., Letu, H., Su, Y., Chen, T., Wu, X. (2019), Fifteen-year statistical analysis of cloud characteristics over China using Terra and Aqua MODIS observations. *International Journal of Climatology*, 38(5), 2612–2629. <https://doi.org/10.1002/joc.5975>
- Zhao, C., Yang, Y., Fan, H., Huang, J., Fu, Y., Zhang, X., Kang, S., Cong, Z., Letu, H., Menenti, M. (2020), Aerosol characteristics and impacts on weather and climate over the Tibetan Plateau. *National Science Review*, 7, 492–495. <https://doi.org/10.1093/nsr/nwz184>
- Zhao, P., Xiao, H., Liu, J., Zhou, Y. (2022), Precipitation efficiency of cloud and its influencing factors over the Tibetan plateau. *International Journal of Climatology*, 42(1), 416–434. <https://doi.org/10.1002/joc.7251>
- Zhang, Z., Ackerman, A. S., Feingold, G., Platnick, S., Pincus, R., Xue, H. (2012), Effects of cloud horizontal inhomogeneity and drizzle on remote sensing of cloud droplet effective radius: Case studies based on large-eddy simulations. *Journal of Geophysical Research: Atmospheres*, 117, D19208. <https://doi.org/10.1029/2012JD017655>
- Zhu, J., Xia, X., Che, H., Wang, J., Cong, Z., Zhao, T., Kang, S., Zhang, X., Yu, X., Zhang, Y. (2019), Spatiotemporal variation of aerosol and potential long-range transport impact over the Tibetan Plateau, China. *Atmospheric*

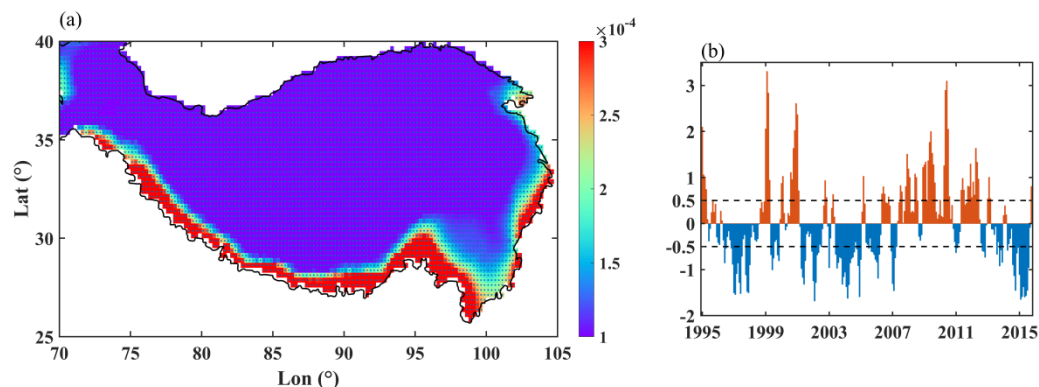


Figure 1. Trends of AI (month⁻¹) (a) and time series of AI anomaly from 1995 to 2015 (b), processed by removing the annual cycle and linear trend and standardizing. The dashed lines indicate thresholds for positive and negative AI events.

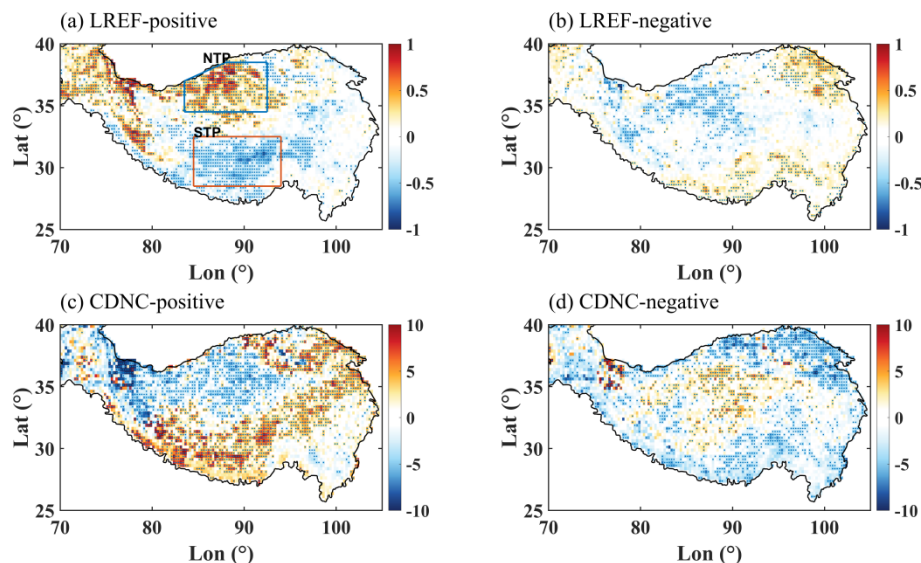


Figure 2. Composite LREF anomalies (m) for positive (a) and negative (b) AI events, and composite CDNC anomalies (cm⁻³) for positive (c) and negative (d) AI events in the warm season from 1995 to 2015 over the TP. Dot symbols in the grid indicate that a 95% significance level has been passed according to the Student's *t*-test. The blue and red boxes represent the NTP and STP, respectively.

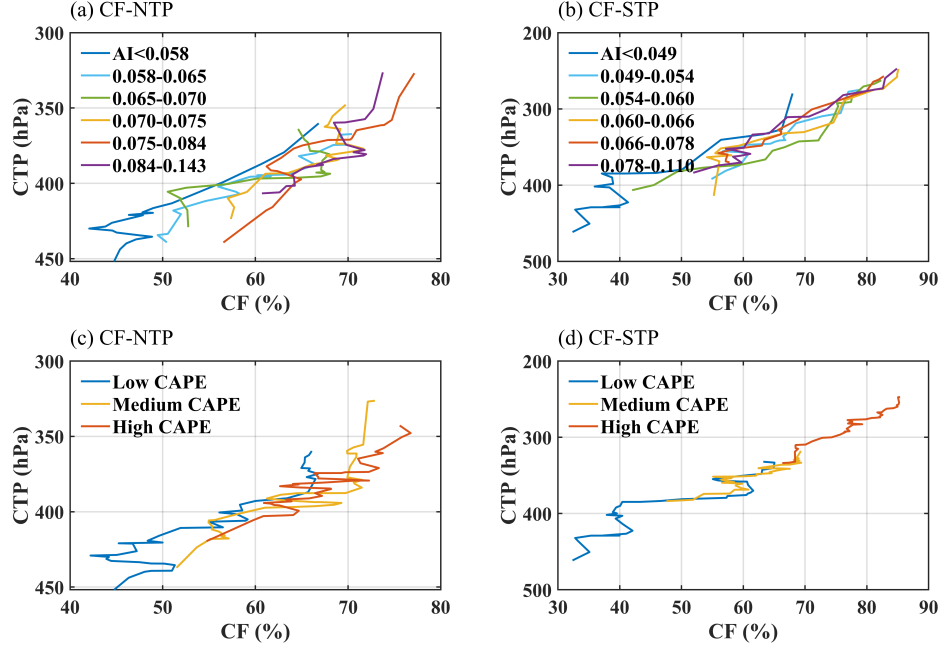


Figure 3. CF as a function of CTP in the warm season. CFs are grouped into 6 groups according to AI over the NTP (a) and STP (b); and CFs are grouped into 3 classes according to the CAPE over the NTP (c) and STP (d).

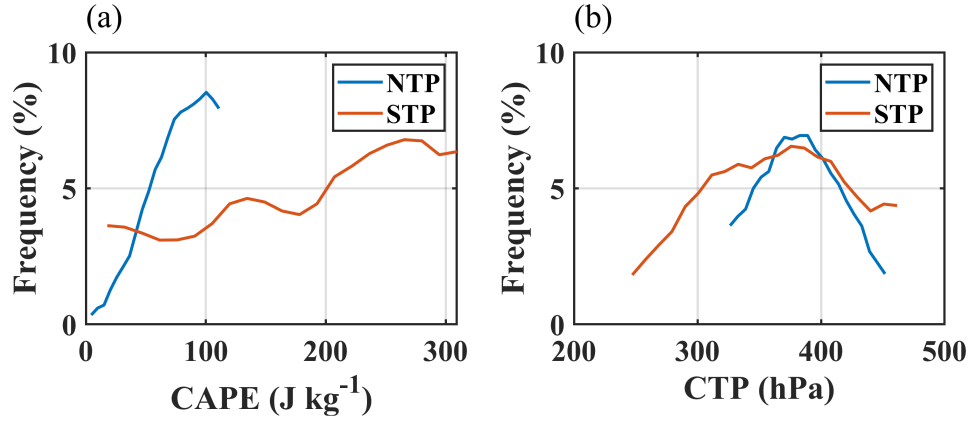


Figure 4. The occurrence frequency of CAPE and CTP over the NTP and STP in the warm season.

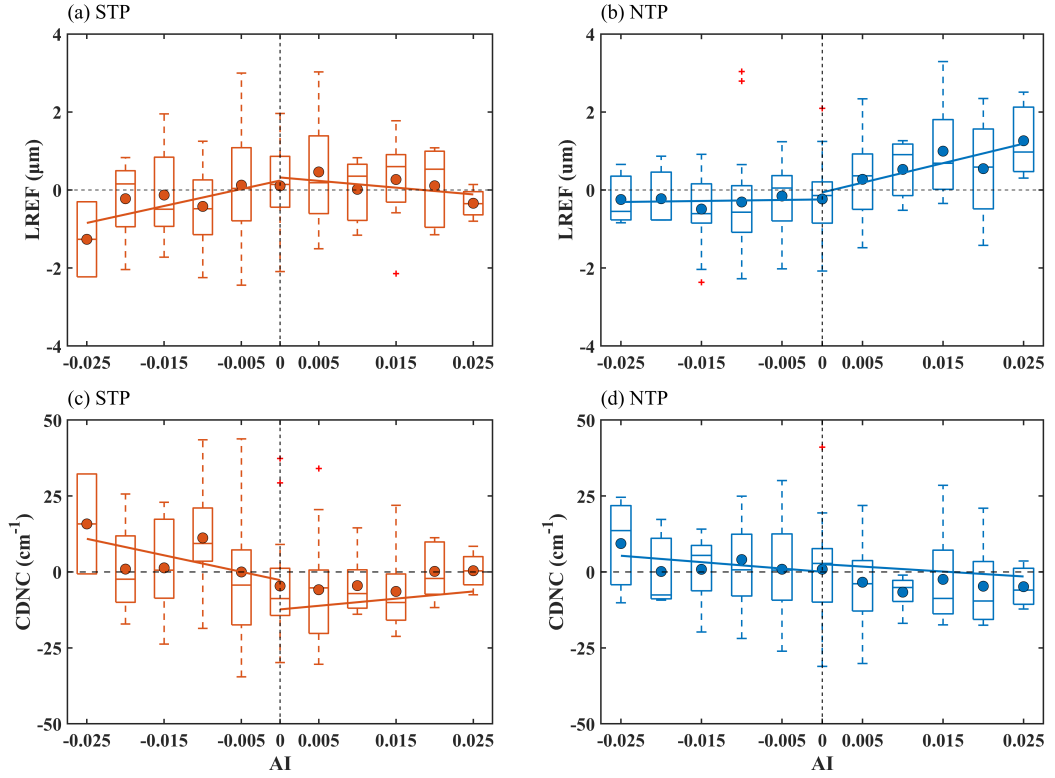


Figure 5. The variation of LREF (m) and CDNC (cm⁻³) anomalies with AI anomaly over the NTP and STP in the warm season.

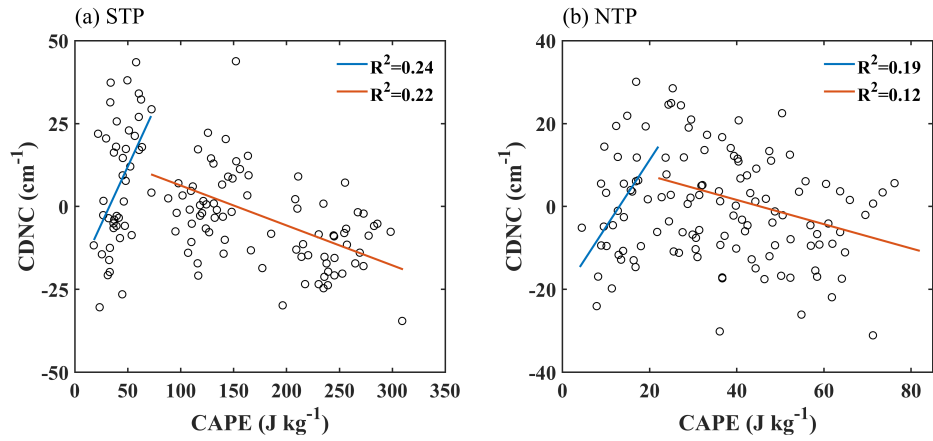


Figure 6. Variation of CDNC anomaly with CAPE in the warm season over the STP (a) and NTP (b).

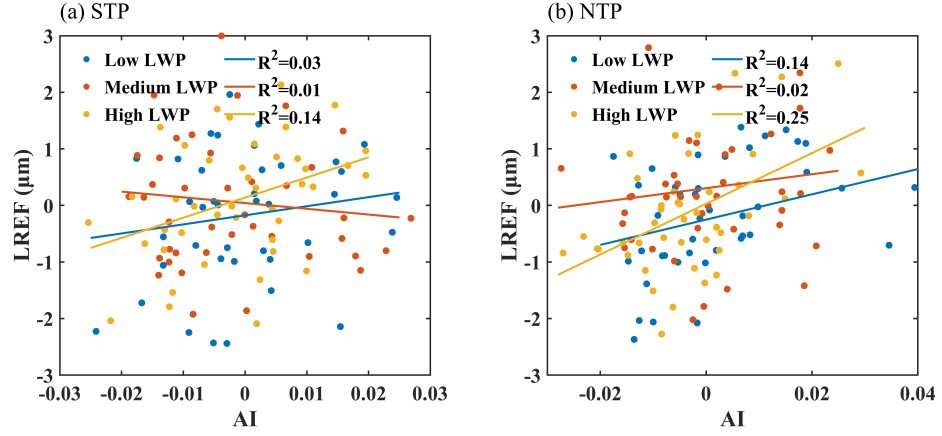


Figure 7. Variation of LREF anomaly with AI anomaly under different LWP conditions over the STP (a) and NTP (b) in the warm season.

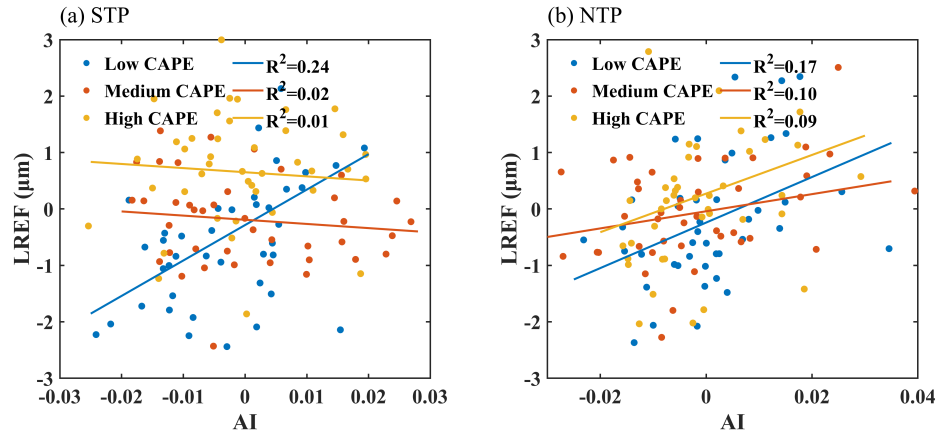


Figure 8. Variation of LREF anomaly with AI anomaly under different CAPE conditions over the STP (a) and NTP (b) in the warm season.

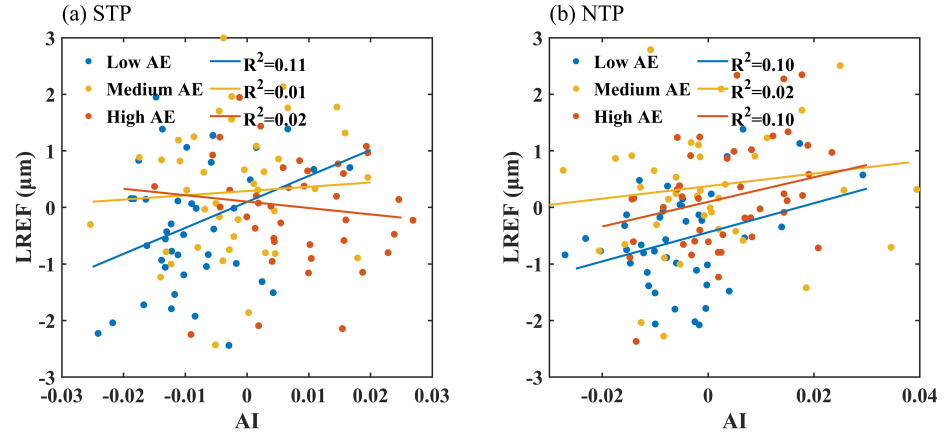


Figure 9. Variation of LREF anomaly with AI anomaly under different AE conditions over the STP (a) and NTP (b) in the warm season.